Water Research 262 (2024) 122094

Contents lists available at ScienceDirect

Water Research

journal homepage: www.elsevier.com/locate/watres

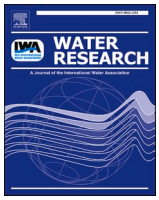

Transformation of sedimentary dissolved organic matter in electrokinetic remediation catalogued by FT-ICR mass spectrometry

Tahir Maqbool [a], Huan Chen [b], Qingshi Wang [a], Amy M. McKenna [b,c], Daqian Jiang [a,*]

[a] Department of Civil, Construction, and Environmental Engineering, The University of Alabama, Tuscaloosa, AL, 35487, USA
[b] National High Magnetic Field Laboratory, Florida State University, 1800 East Paul Dirac Dr., Tallahassee, FL, 32310-4005, USA
[c] Department of Soil and Crop Sciences, Colorado State University, Fort Collins, CO, 80523, USA

ARTICLE INFO

Keywords:
Electrokinetic remediation
Dissolved organic matter
FT-ICR MS
High-resolution mass spectrometry
Metagenomic sequencing

ABSTRACT

In electrokinetic remediation (EKR), the sedimentary dissolved organic matter (DOM) could impede remediation by scavenging reactive species and generating unintended byproducts. Yet its transformation and mechanisms remained largely unknown. This study conducted molecular-level characterization of the water-extractable DOM (WEOM) in EKR using negative-ion electrospray ionization coupled to 21 tesla Fourier transform ion cyclotron resonance mass spectrometry (21 T FT-ICR MS). The results suggested that ~55 % of the ~7,000 WEOM compounds identified were reactive, and EKR lowered their diversity, molecular weight distribution, and double-bond equivalent (DBE) through a combination of electrochemical and microbial redox reactions. Heteroatom-containing WEOM (CHON and CHOS) were abundant (~ 35% of the total WEOM), with CHOS generally being more reactive than CHON. Low electric potential (1 V/cm) promoted the growth of dealkylation and desulfurization bacteria, and led to anodic CO_2 mineralization, anodic cleavage of -SO and -SO_3, and cathodic cleavage of -SH_2; high electric potential (2 V/cm) only enriched desulfurization bacteria, and differently, led to anodic oxygenation and cathodic hydrogenation of unsaturated and phenolic compounds, in addition to cathodic cleavage of -SH_2. The long-term impact of these changes on soil quality and nitrogen-sulfur-carbon flux may be need to studied to identify unknown risks and new applications of EKR.

1. Introduction

Contaminated sediments are ubiquitous in the U.S., with 1,337 sites recently added to the Environmental Protection Agency (EPA) National Priorities Sites (US-EPA, 2021). Due to the high concentrations of pollutants and the risk of propagation through food chains (e.g., contaminated sediment in Guánica Bay, Puerto Rico, contained a high polychlorinated biphenyls level of 129,300 ng/g and fish samples showed absorption in range of 1,623 ng/g to 3,768 ng/g) (Kumar et al., 2016), mitigation of contaminated sediments has been a key target in the EPA's programs such as the Superfund and Great Lakes Legacy Acts (U.S. EPA, 2021). For instance, in the state of Ohio alone, 1.5 million tons of sediment are dredged annually from its ports for pollution prevention (https://lakeerie.ohio.gov/); an estimated $900 million is needed for the remediation of 5 million m^3 sediments in the Detroit River contaminated with industrial discharge (https://www.greatlakessnow.org/).

Remediation of contaminated sediments generally has been challenging due to large variations in sediment properties (e.g., structure, pH, and salinity) (Alori et al., 2022; Klik et al., 2020), interfacial chemistry, and contamination types/levels (Benamar et al., 2020; Bergen et al., 2005; Bolan et al., 2023; Zhang et al., 2016). Among the available practices, electrokinetic remediation (EKR) has shown effectiveness toward different sediment compositions (e.g., clay and sandy) (Alcántara et al., 2012; Virkutyte et al., 2002) and contaminants (e.g., organic and inorganic) with the advantages of being chemical-free and achieving relatively fast kinetics (Guedes et al., 2014; Maini et al., 2000; Wen et al., 2021). Driven by an electric potential, EKR achieves remediation through a combination of translocation (i.e., electroosmosis, electromigration, and electrophoresis), and electrochemical transformation (e.g., electrolysis at electrode surfaces) (Acar et al., 1995; Chen et al., 2021).

Contrasting the abundance of interest in characterizing the fate of contaminants in EKR (Liu et al., 2022; Maqbool and Jiang, 2023; S. Wang et al., 2016; Zheng et al., 2021), how EKR alters sedimentary properties, particularly the dissolved organic matter (DOM), is not

* Corresponding author.
E-mail address: daqian.jiang@ua.edu (D. Jiang).

https://doi.org/10.1016/j.watres.2024.122094
Received 16 May 2024; Received in revised form 27 June 2024; Accepted 12 July 2024
Available online 30 July 2024

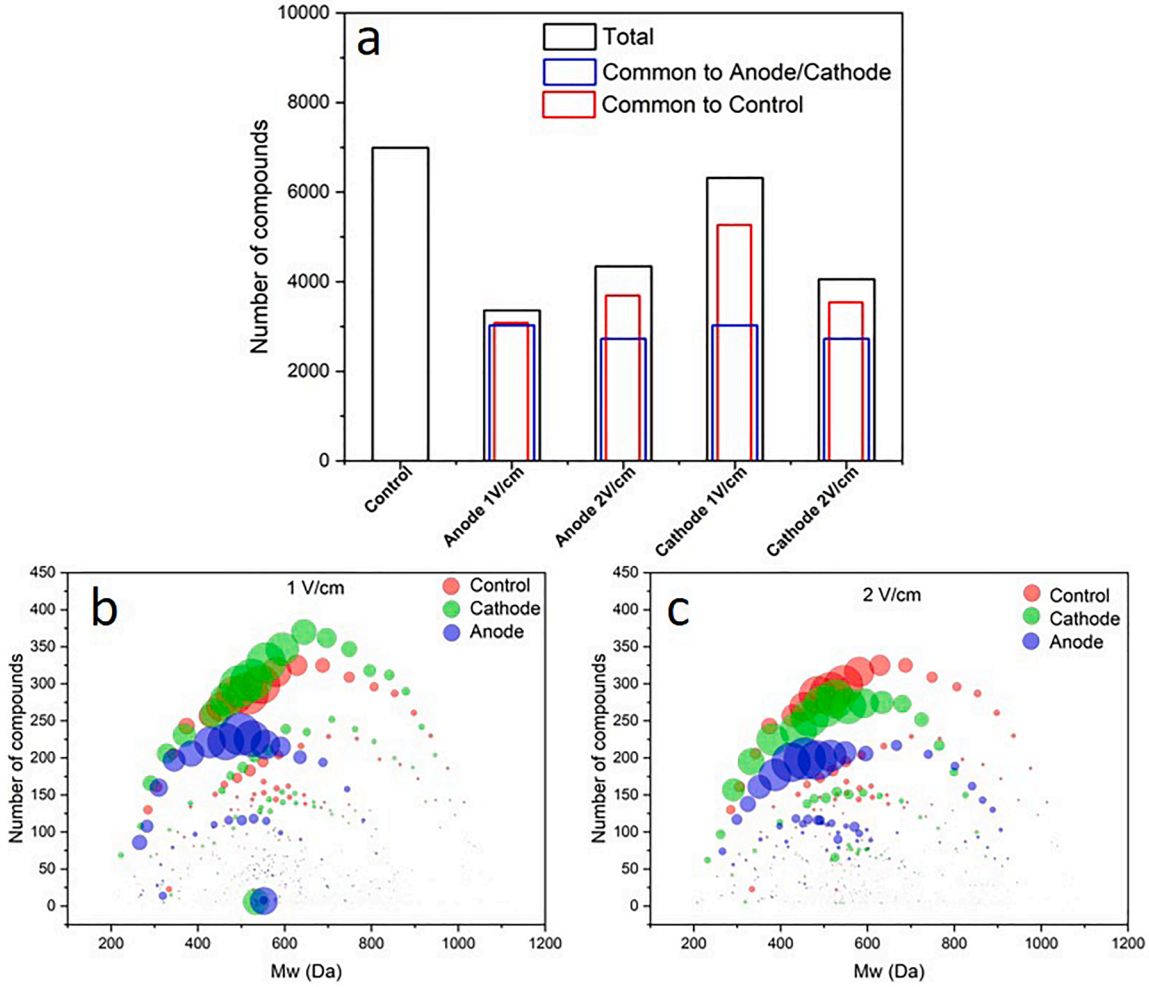

Fig. 1. (a) The total number of unique compounds in sediment WEOM from the control reactor, anode, and cathode of EKRs working at 1V/cm and 2V/cm. The blue column represents the number of compounds shared with the counter electrode (e.g., for Anode 1V/cm, it's the number of compounds also detected in Cathode 1V/cm) and the red column represents the number of compounds shared with the Control. The total number of unique compounds is the sum of organic compounds containing CHO, CHON, and CHOS. Distribution of WEOM compounds with respect to molecular weight (Mw; Da) in (b) EKR1V and (c) EKR2V. The bubble size represents the intensity of weight fractions and is not comparable across figures.

well-understood (Alshawabkeh, 2009; Fan et al., 2022). Sedimentary DOM, a heterogeneous matrix with abundant refractory humic substances of varying size and aromaticity (Chen and Hur, 2015; Hur et al., 2014), contains thousands of compounds ranging from polyphenols, unsaturated and phenolic compounds, to aliphatic compounds, with varying levels of double-bond equivalent (DBE) and aromaticity (Bahureksa et al., 2021; Schmidt et al., 2011; Xu et al., 2016). It is a critical factor that impacts the water holding capacity, contaminant mobility, and substrate availability for microorganisms in sediments (Ren et al., 2015; L. Zhang et al., 2022). Heteroatom (N, S, and P) containing DOM are sources of essential nutrients for the benthic community, controlling the biogeochemical cycling of essential elements (Ksionzek et al., 2016; McCarthy et al., 1997). Preliminary evidence suggests that remediation systems (Fox et al., 2017; McKee and Hatcher, 2015), particularly EKR, could significantly alter the composition of DOM through, for example, degradation and translocation of DOM coupled with over 100-fold changes in the aromaticity and microbially degradable nonaromatic constituents (Maqbool and Jiang, 2023). Such changes may impact the benthic flux of nutrients and carbon post-remediation and, in turn, change the benthic ecosystems (Dadi et al., 2016; Yang et al., 2014).

Herein, we provided the first molecular-level characterization of the transformation of sedimentary DOM in EKR enabled by 21 tesla Fourier-transform ion cyclotron resonance mass spectrometry (21T FT-ICR MS). FT-ICR MS at 21 tesla is the only mass analyzer with the resolving power to separate species that differ in mass by the mass of an electron across a wide molecular weight range (m/z 150-1500), a fundamental requirement for polydispsere, polyfunctional complex organic mixtures (e.g., DOM). Coupled with negative-ion electrospray ionization that yields deprotonation of acidic functional groups prevalent in DOM, more than 30,000 unique elemental compositions from a single DOM extract were identified across a wide continuum of molecular weight, aromaticity, double bond equivalents (DBE), elemental composition (e.g., heteroatoms), and functional groups (Bahureksa et al., 2022; Hendrickson et al., 2015). By characterizing sedimentary DOM in different EKR and control conditions at this resolution, we aimed to shed new light on the impacts and safety of EKR to inform further research and development.

2. Material and method

2.1. Sample collection and reactor setup

The sediments were sampled from the bank of Lake Tuscaloosa (Alabama, USA), transferred to the laboratory immediately, sieved (<2 mm), and homogenized thoroughly before the experiment (sediment characteristics are presented in **Table S1**). The 5,885-acre lake serves as

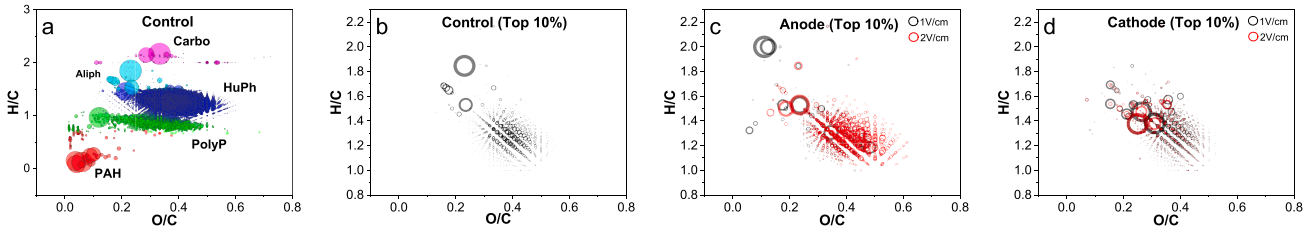

Fig. 2. (a) Distribution of polyaromatic hydrocarbons (PAH), polyphenol (PolyP), highly unsaturated and phenolics (HuPh), aliphatic (Aliph), and carbohydrates (Carbo) in WEOM in the control reactor as shown in a Van Krevelen diagram. Van Krevelen diagrams of compounds with top 10 % intensity in the control reactor (b), EKR anodes (c), and EKR cathodes (d).

the primary drinking water source for the region (https://www.tuscaloosa.com). EKR comprised plastic reactors (33 × 16 × 11 cm) with removable lids and holes for the electrodes (**Fig. S1**). The graphite electrodes (15 × 7.6 × 0.6 cm) (**Table S2**) were inserted into sediments. The inter-electrode distance was maintained at 15 cm. In each reactor, sediments were mixed with ultrapure water (UPW) at 2:1 and left overnight. EKR was duplicated under three different conditions: 0V/cm (control), 1 V/cm (EKR1V), and 2 V/cm (EKR2V). The absolute DC potentials applied across electrodes were 15V and 30V for EKR1V and EKR2V, respectively. EKRs were operated for four weeks which stabilized the pH at electrodes. Sediment samples were collected from two locations, cathode and anode, for DOM characterization.

2.2. Extraction of DOM

DOM samples for FT-ICR MS characterization were collected after the stabilization of the EKR. DOM was extracted as water-extractable organic matter (WEOM) by mixing the sediments with UPW (10:1), shaking overnight at 200 rpm, and centrifuging at 6,000 rpm for 15 min at 4°C. WEOM supernatant were filtered through 0.45 μm membrane filters (Fisherbrand, USA).

Before the solid phase extraction (SPE), all the WEOM solutions were acidified (pH = 2) (Dittmar et al., 2008). The 6 mL and 1 g resin SPE cartridges (Bond Elut Cartridge-PPL, Agilent) were used to extract WEOM. Briefly, SPE cartridges were rinsed (UPW; 15 mL), followed by activation (methanol; 15 mL). SPE cartridges were mounted on the manifold and loaded with ~700 mL of WEOM samples with a flow speed of 5 mL min^{-1}. The cartridges were desalted with 15 mL of 0.01 M HCl and gently dried the cartridges using nitrogen (N_2) flow. In the end, WEOM retained was eluted using 15 mL of methanol, concentrated to 1 mL in an N_2 concentrator, and stored at -20°C before FT-ICR MS measurements (He et al., 2016; Kurek et al., 2020).

2.3. FT-ICR MS analysis

The details of the FT-ICR MS analysis are provided in the SI. Only the non-halogenated WEOM were included in this study. The halogenated WEOM were analyzed in a separate study. WEOM solution was infused via a microelectrospray source at 500 nL/min by a syringe pump (Emmett et al., 1998). The operating conditions, emitter voltage (-2.4-2.9 kV) S-lens RF level (45 %), and heated metal capillary temperature (350 °C), were optimized for negative ion formation: WEOM was analyzed with FT-ICR MS equipped with a 21 tesla superconducting magnet (Hendrickson et al., 2015; Smith et al., 2018).

2.4. Microbial community analysis

Whole genome shotgun sequencing was applied to characterize the microbial community. Sediments samples were collected and preserved at -80 °C before extraction. DNA extraction was performed using ZYMO Quick-DNATM Fecal/Soil Microbe Miniprep Kit D6010 (Zymo Research, Irvine, CA, USA) following prescribed instructions. After detection of the concentration and purity of the extracted DNA. Sequencing libraries of samples were prepared with Illumina® DNA Library Prep Kit (Illumina, San Diego, CA) with up to 500 ng DNA input using unique dual-index 10 bp barcodes with Nextera® adapters (Illumina, San Diego, CA). All libraries were pooled in equal abundance. The final pool was quantified using qPCR and TapeStation® (Agilent Technologies, Santa Clara, CA). The final library was sequenced on Illumina® NovaSeq® (Illumina, San Diego, CA). The ZymoBIOMICS® Microbial Community DNA Standard (Zymo Research, Irvine, CA) was used as a positive control for each library preparation. Negative controls (i.e., blank extraction control, blank library preparation control) were included to assess the level of bioburden carried by the wet-lab process. Microbial composition was profiled with Centrifuge using bacterial, viral, fungal, mouse, and human genome datasets. The sequences reported in this article have been deposited in the NCBI BioProject (accession no. PRJNA1066388).

3. Results

3.1. Electrokinetic remediation (EKR) reduced diversity of water-extractable organic matter (WEOM)

EKR consistently reduced the diversity of WEOM, with no consistent trend identified between the voltage applied and the WEOM diversity. ~7000 elemental compositions of different compounds were identified in the control condition (i.e., sum of three organic compound groups containing CHO, CHON, and CHOS). In contrast, the total number was only 3300-6300 under electrokinetic conditions (Fig. 1**a, Table S3**). Cathode 1V/cm had the highest number of compounds (~6300), 88 % higher than the lowest Anode 1V/cm.

Among the ~7000 compounds identified, ~3000 were shared in all the anodes and cathodes under all the conditions (Fig. 1**a**). Creation of new compounds was limited: 500-1000 new compounds were created, with cathode 1 V/cm and anode 1 V/cm generating the most and fewest new compounds, respectively (Fig. 1**a**).

3.2. Anode yielded smaller-sized compounds

EKR anode reduced the average molecular weight (Mw) of WEOM compared to the control reactor, whereas EKR cathode did not lead to significant changes (Fig. 1**b-c**). While WEOM in all the reactors contained a wide size range (Mw; 200-1000 Da), EKR anode was characterized by intense peaks below 450 Da, and the control and EKR cathode showed intense peaks above 500 Da (Fig. 1**b-c**). The difference in average molecular weight between EKR1V and EKR2V was ≤5 %.

3.3. Anodic oxygenation and cathodic hydrogenation of WEOM

Similar to previous reports, (Lv et al., 2016; Šantl-Temkiv et al., 2013) WEOM in the control reactor was composed of compounds from five different classes: polyaromatic hydrocarbons (PAH), polyphenol (PolyP), highly unsaturated and phenolics (HuPh), aliphatic (Aliph), and carbohydrates (Carbo) (**Fig. S2**). HuPh and Aliph dominated, HuPh (78 %)> Aliph (10 %)> PolyP (6 %)> Carbo (2 %)>PAH (1 %) (Fig. 2**a** and **Fig. S3**), with O/C and H/C in the ranges of 0.1 to 0.5 and 0.8 to 2.0,

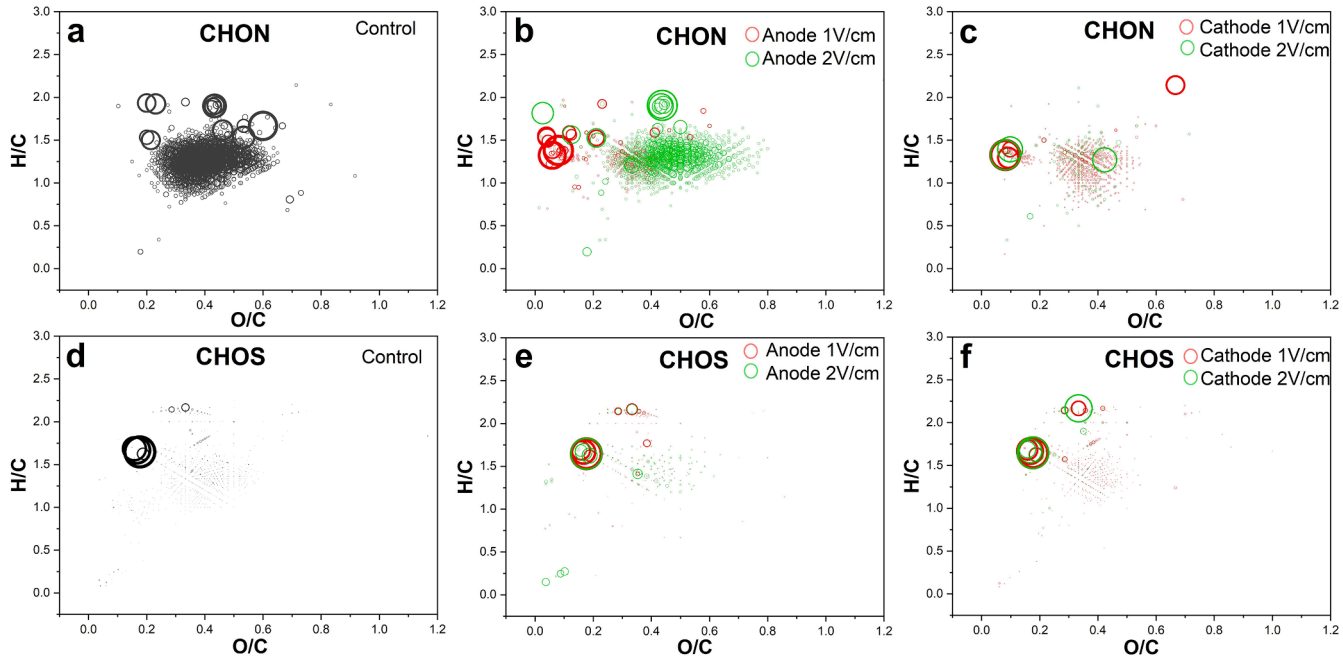

Fig. 3. Distribution of N-WEOM (CHON) and S-WEOM (CHOS) in the control reactor (a and d), EKR anodes (b and e), and EKR cathodes (c and f) of the EKRs.

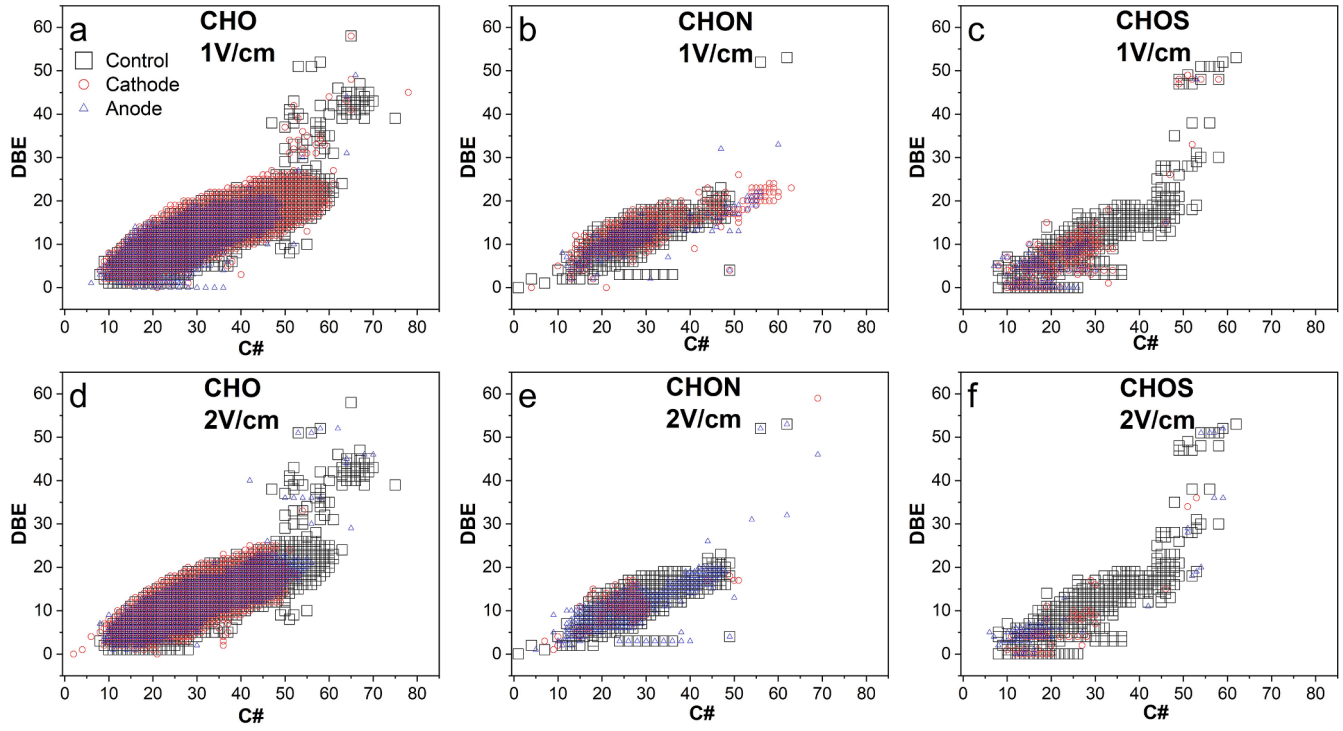

Fig. 4. Distribution of C# (Number of carbon in compounds) vs. double-bond equivalent (DBE) in CHO, CHON, and CHOS in EKR 1V/cm (a-c) and EKR 2V/cm (d-f).

respectively (Fig. 2**b**).

EKR anode showed voltage-dependent impacts on the composition of WEOM. Anode 2V/cm generated compounds with higher O/C (0.4 to 0.6, 15 % higher than the control reactor) and contained over 40 % unique HupH (Fig. 2**c**). In contrast, anode 1V/cm did not show noticeable oxidation of HupH (as evidenced by the unchanged O/C and H/C), but generated carbohydrates with higher H/C >1.8.

EKR cathode, regardless of the voltage, generated Aliph with lower H/C. Unlike the control reactor, high-intensity compounds with O/C ~0.2 and H/C ~1.8 were undetected, and new high-intensity compounds emerged with O/C ~0.3 and H/C 1.4 (Fig. 2**b** and 2**d**). Other DOM components (Carbo, PAH, and PolyP) did not make up significant shares at the EKR cathode.

3.4. Degradation of S-WEOM and translocation of N-WEOM under 2 V/cm

1 V/cm degraded WEOM containing CHON and CHOS at both the anode and the cathode, while 2 V/cm degraded CHOS and accumulated CHON at the anode (Fig. 3). CHON and CHOS comprised 16.7 % and

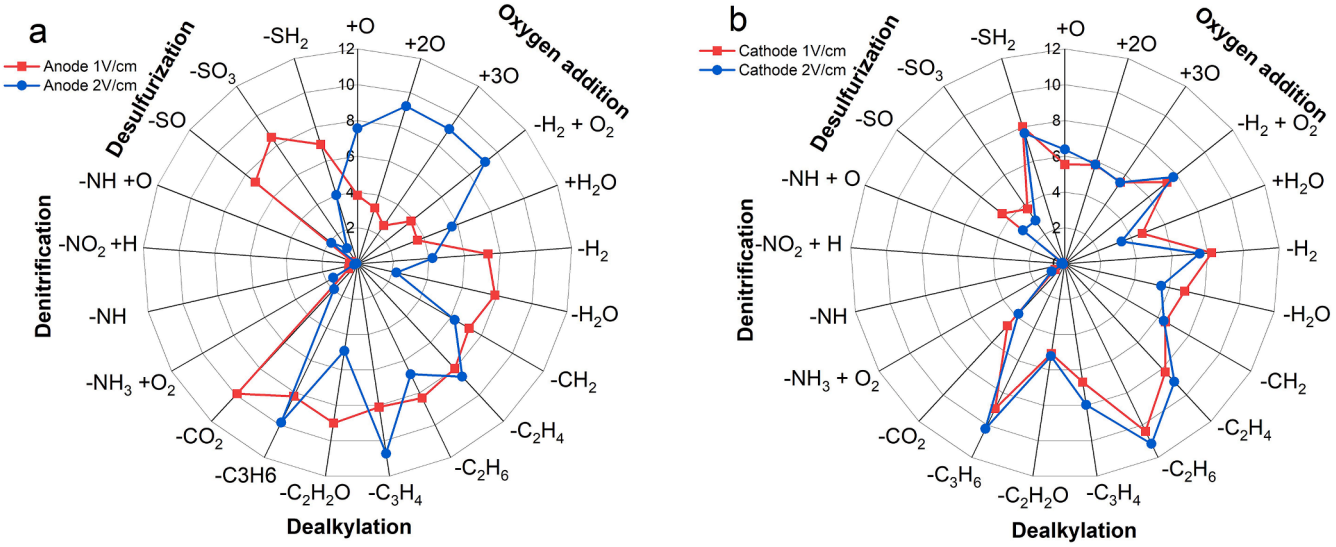

Fig. 5. The number of possible precursor-product pairs (%) between precursors (control WEOM) and products (unique compounds at anodes (a) and cathodes (b)) in EKR. The classes of precursor-product pairs were defined based on the literature (Hou et al., 2022; Zhang et al., 2021).

10.5 % of the WEOM in the control reactor but decreased to 9.2-10.5 % and 4.9-6.0 %, respectively, under 1 V/cm (**Table S3**). Under 2 V/cm, CHOS decreased consistently to 1.5-1.7 %, but CHON increased to 24 % at the anode while decreasing to 2.8 % at the cathode (**Table S3**).

There was no significant change in the H/C and O/C ratios in the CHON and CHOS during EKR, except for the O/C ratios of CHON, which decreased from 0.40 in the control reactor to 0.04, 0.30, and 0.26 under 1 V/cm cathode, 2 V/cm cathode and 1 V/cm anode respectively (Fig. 3 and **Table S3**). 2 V/cm anode increased the O/C ratio slightly to 0.45 (**Table S3**).

3.5. Saturation of N- and S-WEOM

EKR led to shortening of WEOM under all the conditions at both electrodes, but DBE reductions were impacted the elemental composition (Fig. 4). Among the WEOM classes, CHO (WEOM without heteroatoms) have shown the highest reduction (31-46 %) in DBE, followed by CHOS (15-42 %), and CHON (-3 to17 %) (**Table S3**). The reductions in carbon chain length in CHO (32-44 %) and CHON (3-18 %) were proportional to the decrease in DBE except for CHOS, which showed a less significant reduction of carbon chain length than that of DBE.

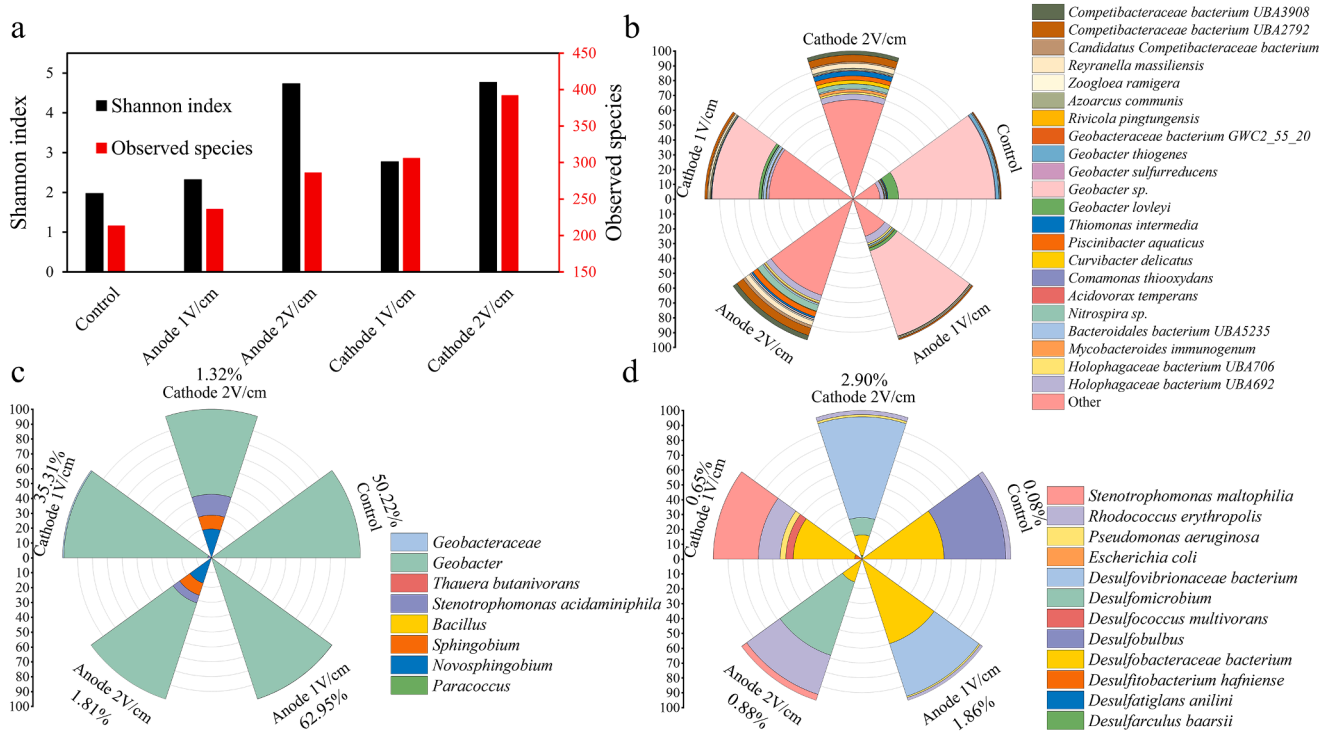

Fig. 6. Microbial communities of EKR. (a) alpha diversity (Shannon) index and total number of species; (b) dominant species in each condition (species with relative abundance less than 2 % were not shown); relative abundances of known (c) dealkylation and (d) desulfurization species or genera normalized to respective totals. Numbers in c) and d) represent the relative abundances of these species/genera in the entire community.

Anode showed higher reductions in DBE and carbon chain length across all the elemental compositions (CHO, CHON and CHOS) than cathode, but different elemental compositions responded differently to the voltage applied. The DBE of CHO and CHOS at anode 2V/cm were 8 % and 32 % higher than anode 1V/cm, respectively, whereas the DBE of CHON at anode 2V/cm was 9 % lower than anode 1V/cm. Cathode 2V/cm showed consistently lower DBE than cathode 1V/cm for all the elemental compositions. The highest DBE (14.0) was observed at cathode 1V/cm for CHO, while the lowest DBE (11.3) was recorded at cathode 2V/cm for CHOS.

3.6. Anodic oxygenation and desulfurization under 2 V/cm and 1 V/cm, respectively

EKR produced ~900 to ~4900 precursor-product pairs, with the highest being cathode 1V/cm and the lowest being anode 1V/cm (Fig. 5). At anode, 1 V/cm facilitated cleavage of -SO, -SO_3, -SH_2, -C_2H_2O, -H_2, and -COO (Fig. 5**a**), while 2 V/cm facilitated oxygenation (+O, +2O, +3O and -H_2+O_2). Cathode was dominated by cleavages of -SH_2, -C_3H_6, -C_2H_8, -H_2 and -H_2+O_2, with voltage having limited impacts (Fig. 5**b**).

3.7. Microbial community enrichment and abundant desulfurizing species

Intense EKR conditions raised the diversity of the microbial communities, as evidenced by the 2-fold increase in the Shannon index in EKR2V at both anode and cathode (Fig. 6**a**). Cathode, in particular, almost doubled the total number of microbial species compared to the control condition (Fig. 6**a**). The species-level community composition is provided in Fig. 6**b**.

The dealkylation species were enriched only under 1 V/cm, while the desulfurization species were enriched under both 1 V/cm and 2 V/cm. For instance, the relative abundance of dealkylation species were 63 % and 2 % of the entire community at 1V/cm and 2V/cm anodes respectively, while 23- and 36-fold increases in the relative abundance of desulfurization speces were noted at 1V anode and 2V cathode respectively (Fig. 6**c and d**). New dealkylation species (*Stenotrophomonas acidaminiphila, Thauera Butanivorans* and species from genus *Sphingobium)* emerged at the higher potential of 2 V/cm (Chen et al., 2023; Li et al., 2019), albeit in low relative abundances. *Rhodococcus erythropolis* and *Pseudomonas aeruginosa* (Denis-Larose et al., 1997; Duarte et al., 2001), bacteria from family Desulfobacteraceae and Desulfovibrionaceae, and species from genus *Desulfovibrio* (Karnachuk et al., 2021; Kümmel et al., 2015), all known desulfurization species, were enriched in EKR (Fig. 6**d**).

4. Discussion

Our results suggest that ~55 % of the ~7000 WEOM compounds were reactive and mobile in EKR, but the generation of new compounds was limited (500-1000 new compounds generated, Fig. 1). The translocation of WEOM was driven by electroosmosis towards the cathode and electromigration of HuPh towards the anode, as suggested previously (Liu et al., 2022; Xu et al., 2014). The transformation of WEOM was dominated by anodic cleavage of large compounds and oxidation of double bonds, which led to a 10 % decrease in anode Mw (Fig. 1**b-c**) and a 12 % decrease in DBE overall. Anodic dealkylation and desulfurization at 1V/cm were likely driven by microbial activity (Fan et al., 2022), as evidenced by the enrichment of dealkylation and desulfurization microorganisims (Fig. 6). Anodic oxygenation was likely driven by electrochemical oxidation (Li et al., 2001), as evidenced by the preference for 2 V/cm and the significant decrease in the abundance of dealkylation species at 2 V/cm. Cathodic -SH_2 cleavage and cathodic dealkylation were similar under 1 V/cm and 2 V/cm, and the distinct microbial community structures (Fig. 6) possibly suggested that electrochemical redox was the dominant pathway (Fliermans and Brock, 1972; Zhang et al., 2022).

We suggest that two WEOM groups are of particular importance in EKR:

Highly unsaturated and phenolic compounds (HupH): 85 % of the total WEOM compounds in sediment belonged to the HupH class. Cathodes led to a higher pH through water electrolysis (**Fig. S4**), which likely enhanced the dissolution and electroosmosis of HuPh due to the presence of carboxylic acid groups in HuPh (as characterized by the IR spectra) (Maqbool and Jiang, 2023). The carboxylic acid groups either migrated to the anode through electromigration (Han et al., 2021) or underwent electrochemical reduction at the cathode. The cathodic electrochemical reduction was possibly mainly hydrogenation and relatively weak, as evidenced by the slight increase in H/C (up to 5 % increase in H/C of the most abundant compounds) in this work and others (Deng et al., 2019). The carboxylic groups that migrated to the anode likely contributed to the higher O/C and lower DBE (Maqbool et al., 2022), as it has been reported that lower pH at the anode causes the generation of H^+, which acts as a mediator between the electrode surface and reactants and facilitates electroxation (WEOM) (Xu et al., 2014).

Heteroatoms-containing WEOM: Over 35 % of the WEOM contained heteroatoms N or S. These N- and S-containing WEOM (CHON and CHOS) were more reactive than those with only CHO (Laszakovits et al., 2020), likely due to their highly reactive functional groups (e.g., -NO_2 and –SH) (Zhang et al., 2021),(Geneste, 2018; Kaboudin et al., 2022; Popp and Schultz, 1962). In EKR, CHOS were highly reactive, whereas CHON were less reactive and accumulated at the anode under 2 V/cm. Both were possibly transformed to CHO with lower DBE. Despite the significant degradation of CHON, the precursor-pairs approach identified limited cleavage of -NH, -NH_3, and -NO_2, suggesting that N removal was either attributable to substitutions by other elements (e.g., halides) (Essaïed et al., 2022; Lee et al., 2007) or accompanied by C-C chain shortening.

Future work: This study, for the first time, reports molecular-level insights into how electrokinetic remediation transforms the dissolved sedimentary organics through electrochemical redox and microbial activities. It should be noted that other factors may also impact the fate of organics. For example, metals in the sediment may influence the mobility and biodegradation of labile organics and also affect their chemical reactivity (Fan et al., 2023; Feng and Ni, 2024; Wang et al., 2024; Yuan et al., 2018). Organics degradation and reactivity are also subject to sediment temperature (Tabuchi et al., 2010; Y. Wang et al., 2016). In-situ or field applications of EKR could cause sediment to heat up, which might influence the dissolution, biodegradability, and electrochemical reactivity of the dissolved organic matter (Guedes et al., 2019; Kim et al., 2012). Future work could explore these important parameters.

Further, the mechanisms of electrochemical redox reactions in EKR remain unclear. EKR produce H_2O_2 at the surface of electrodes, which could interact with metals species in sediment and generate hydroxyl radical, one of reactive oxygen species (ROS) that could degrade organics (Pourfadakari et al., 2021). Redox active moieties of DOM have also been reported to drive direct exchange of electrons at electrodes in electrochemical systems (Ju et al., 2023; Yuan et al., 2011). However, direct evidence on both mechanisms is lacking (Guedes et al., 2014; Pourfadakari et al., 2021). Controlled experiments and direct measurements of ROS could be explored for clarifications.

5. Conclusion

This work demonstrates molecular-level changes in the water-extractable organic matter (WEOM) of sediment in electrokinetic remediation (EKR). While electric potential and existence of heteroatoms (N and S) impact WEOM transformation, in general, anodic

oxidation is dominated by microbial CO_2 elimination at the lower potential of 1 V/cm and electrochemical oxygen addition at the higher potential of 2 V/cm. Cathodic reduction is dominated by dealkylation at both low and high potentials. As a result, EKR-remediated sediments may contain more saturated WEOM and less organic N and S. This change in composition could imply lower metal binding capacity with less labile organic substrates and organic nutrients for heterotrophic microorganisms. The long-term impact of this change on nitrogen-sulfur-carbon fluxes at the water-sediment interface may need to be examined carefully to inform large-scale adoption of electrified soil or sediment treatment.

CRediT authorship contribution statement

Tahir Maqbool: Writing – original draft, Visualization, Project administration, Methodology, Investigation, Formal analysis, Data curation, Conceptualization. **Huan Chen:** Writing – review & editing, Validation, Software, Formal analysis, Data curation. **Qingshi Wang:** Writing – original draft, Visualization, Methodology, Data curation. **Amy M. McKenna:** Writing – review & editing, Visualization, Methodology, Funding acquisition, Formal analysis, Data curation. **Daqian Jiang:** Writing – review & editing, Writing – original draft, Validation, Supervision, Project administration, Methodology, Investigation, Funding acquisition, Data curation, Conceptualization.

Declaration of competing interest

The authors declare that they have no known competing financial interests or personal relationships that could have appeared to influence the work reported in this paper.

Data availability

All FT-ICR MS spectra files (.pfd) and elemental composition assignments (.xls) are publicly-available via the Open Science Framework (https://osf.io/6ucjd/) at doi:10.17605/OSF.IO/6UCJD in accordance with the NHFML and NSF FAIR data management plan (https://nationalmaglab.org/images/user_resources/searchable_docs/request_magnet_time/data_management_plan_policy.pdf).

Acknowledgment

We acknowledge financial support by the United States Department of Agriculture (Award Number 2017-67030-27659) and the National Science Foundation (NSF Award Number 2305141). The work conducted at the National High Magnetic Field Laboratory receives support from the NSF Division of Chemistry and Division of Materials Research through DMR-2128556, and the State of Florida.

Supplementary materials

Supplementary material associated with this article can be found, in the online version, at doi:10.1016/j.watres.2024.122094.

References

Acar, Y.B., Gale, R.J., Alshawabkeh, A.N., Marks, R.E., Puppala, S., Bricka, M., Parker, R., 1995. Electrokinetic remediation: Basics and technology status. J. Hazard. Mater. 40, 117–137. https://doi.org/10.1016/0304-3894(94)00066-P.

Alcántara, M.T., Gómez, J., Pazos, M., Sanromán, M.A., 2012. Electrokinetic remediation of lead and phenanthrene polluted soils. Geoderma 173–174, 128–133. https://doi.org/10.1016/j.geoderma.2011.12.009.

Alori, E.T., Gabasawa, A.I., Elenwo, C.E., Agbeyegbe, O.O., 2022. Bioremediation techniques as affected by limiting factors in soil environment. Front. Soil Sci.

Alshawabkeh, A.N., 2009. Electrokinetic Soil Remediation: Challenges and Opportunities. Sep. Sci. Technol. 44, 2171–2187. https://doi.org/10.1080/01496390902976681.

Bahureksa, W., Borch, T., Young, R.B., Weisbrod, C.R., Blakney, G.T., McKenna, A.M., 2022. Improved dynamic range, resolving power, and sensitivity achievable with FT-ICR mass spectrometry at 21 T reveals the hidden complexity of natural organic matter. Anal. Chem. 94, 11382–11389. https://doi.org/10.1021/acs.analchem.2c02377.

Bahureksa, W., Tfaily, M.M., Boiteau, R.M., Young, R.B., Logan, M.N., McKenna, A.M., Borch, T., 2021. Soil organic matter characterization by Fourier transform ion cyclotron resonance mass spectrometry (FTICR MS): a critical review of sample preparation, analysis, and data interpretation. Environ. Sci. Technol. 55, 9637–9656. https://doi.org/10.1021/acs.est.1c01135.

Benamar, A., Ammami, M.T., Song, Y., Portet-Koltalo, F., 2020. Scale-up of electrokinetic process for dredged sediments remediation. Electrochim. Acta 352, 136488. https://doi.org/10.1016/j.electacta.2020.136488.

Bergen, B.J., Nelson, W.G., Mackay, J., Dickerson, D., Jayaraman, S., 2005. Environmental monitoring of remedial dredging at the new Bedford harbor, Ma, superfund site. Environ. Monit. Assess. 111, 257–275. https://doi.org/10.1007/s10661-005-8223-4.

Bolan, S., Padhye, L.P., Mulligan, C.N., Alonso, E.R., Saint-Fort, R., Jasemizad, T., Wang, C., Zhang, T., Rinklebe, J., Wang, H., Siddique, K.H.M., Kirkham, M.B., Bolan, N., 2023. Surfactant-enhanced mobilization of persistent organic pollutants: Potential for soil and sediment remediation and unintended consequences. J. Hazard. Mater. 443, 130189 https://doi.org/10.1016/j.jhazmat.2022.130189.

Chen, M., Hur, J., 2015. Pre-treatments, characteristics, and biogeochemical dynamics of dissolved organic matter in sediments: A review. Water Res. 79, 10–25. https://doi.org/10.1016/j.watres.2015.04.018.

Chen, S.-F., Chen, W.-J., Huang, Y., Wei, M., Chang, C., 2023. Insights into the metabolic pathways and biodegradation mechanisms of chloroacetamide herbicides. Environ. Res. 229, 115918.

Chen, Y., Zhi, D., Zhou, Y., Huang, A., Wu, S., Yao, B., Tang, Y., Sun, C., 2021. Electrokinetic techniques, their enhancement techniques and composite techniques with other processes for persistent organic pollutants remediation in soil: A review. J. Ind. Eng. Chem. 97, 163–172. https://doi.org/10.1016/j.jiec.2021.03.009.

Dadi, T., Friese, K., Wendt-Potthoff, K., Koschorreck, M., 2016. Benthic dissolved organic carbon fluxes in a drinking water reservoir. Limnol. Oceanogr. 61, 445–459. https://doi.org/10.1002/lno.10224.

Deng, W., Xu, K., Xiong, Z., Chaiwat, W., Wang, X., Su, S., Hu, S., Qiu, J., Wang, Y., Xiang, J., 2019. Evolution of aromatic structures during the low-temperature electrochemical upgrading of bio-oil. Energy Fuels 33, 11292–11301. https://doi.org/10.1021/acs.energyfuels.9b03099.

Denis-Larose, C., Labbé, D., Bergeron, H., Jones, A.M., Greer, C.W., Al-Hawari, J., Grossman, M.J., Sankey, B.M., Lau, P.C., 1997. Conservation of plasmid-encoded dibenzothiophene desulfurization genes in several rhodococci. Appl. Environ. Microbiol. 63, 2915–2919.

Dittmar, T., Koch, B., Hertkorn, N., Kattner, G., 2008. A simple and efficient method for the solid-phase extraction of dissolved organic matter (SPE-DOM) from seawater. Limnol. Oceanogr. Methods 6, 230–235. https://doi.org/10.4319/lom.2008.6.230.

Duarte, G.F., Rosado, A.S., Seldin, L., De Araujo, W., Van Elsas, J.D., 2001. Analysis of bacterial community structure in sulfurous-oil-containing soils and detection of species carrying dibenzothiophene desulfurization (dsz) genes. Appl. Environ. Microbiol. 67, 1052–1062.

Emmett, M.R., White, F.M., Hendrickson, C.L., Shi, S.D., Marshall, A.G., 1998. Application of micro-electrospray liquid chromatography techniques to FT-ICR MS to enable high-sensitivity biological analysis. J. Am. Soc. Mass Spectrom. 9, 333–340. https://doi.org/10.1016/S1044-0305(97)00287-0.

Essaïed, K.-A., Brown, L.V., von Gunten, U., 2022. Reactions of amines with ozone and chlorine: Two novel oxidative methods to evaluate the N-DBP formation potential from dissolved organic nitrogen. Water Res. 209, 117864 https://doi.org/10.1016/j.watres.2021.117864.

Fan, R., Tian, H., Wu, Q., Yi, Y., Yan, X., Liu, B., 2022. Mechanism of bio-electrokinetic remediation of pyrene contaminated soil: Effects of an electric field on the degradation pathway and microbial metabolic processes. J. Hazard. Mater. 422, 126959 https://doi.org/10.1016/j.jhazmat.2021.126959.

Fan, T., Yao, X., Sun, Z., Sang, D., Liu, L., Deng, H., Zhang, Y., 2023. Properties and metal binding behaviors of sediment dissolved organic matter (SDOM) in lakes with different trophic states along the Yangtze River Basin: A comparison and summary. Water Res. 231, 119605 https://doi.org/10.1016/j.watres.2023.119605.

Feng, J.-R., Ni, H.-G., 2024. Effects of heavy metals and metalloids on the biodegradation of organic contaminants. Environ. Res. 246, 118069 https://doi.org/10.1016/j.envres.2023.118069.

Fliermans, C.B., Brock, T.D., 1972. Ecology of sulfur-oxidizing bacteria in hot acid soils. J. Bacteriol. 111, 343–350. https://doi.org/10.1128/jb.111.2.343-350.1972.

Fox, P.M., Nico, P.S., Tfaily, M.M., Heckman, K., Davis, J.A., 2017. Characterization of natural organic matter in low-carbon sediments: Extraction and analytical approaches. Org. Geochem. 114, 12–22. https://doi.org/10.1016/j.orggeochem.2017.08.009.

Geneste, F., 2018. Catalytic electrochemical pre-treatment for the degradation of persistent organic pollutants. Curr. Opin. Electrochem. 11, 19–24. https://doi.org/10.1016/j.coelec.2018.07.002.

Guedes, P., Lopes, V., Couto, N., Mateus, E.P., Pereira, C.S., Ribeiro, A.B., 2019. Electrokinetic remediation of contaminants of emergent concern in clay soil: Effect of operating parameters. Environ. Pollut. 253, 625–635. https://doi.org/10.1016/j.envpol.2019.07.040.

Guedes, P., Mateus, E.P., Couto, N., Rodríguez, Y., Ribeiro, A.B., 2014. Electrokinetic remediation of six emerging organic contaminants from soil. Chemosphere 117, 124–131. https://doi.org/10.1016/j.chemosphere.2014.06.017.

Han, D., Wu, X., Li, R., Tang, X., Xiao, S., Scholz, M., 2021. Critical review of electro-kinetic remediation of contaminated soils and sediments: mechanisms, performances and technologies. Water Air Soil Pollut. 232, 335. https://doi.org/10.1007/s11270-021-05182-4.

He, W., Chen, M., Park, J.-E., Hur, J., 2016. Molecular diversity of riverine alkaline-extractable sediment organic matter and its linkages with spectral indicators and molecular size distributions. Water Res. 100, 222–231. https://doi.org/10.1016/j.watres.2016.05.023.

Hendrickson, C.L., Quinn, J.P., Kaiser, N.K., Smith, D.F., Blakney, G.T., Chen, T., Marshall, A.G., Weisbrod, C.R., Beu, S.C., 2015. 21 Tesla Fourier transform ion cyclotron resonance mass spectrometer: a national resource for ultrahigh resolution mass analysis. J. Am. Soc. Mass Spectrom. 26, 1626–1632.

Hou, C., Chen, L., Dong, Y., Yang, Y., Zhang, X., 2022. Unraveling dissolved organic matter in drinking water through integrated ozonation/ceramic membrane and biological activated carbon process using FT-ICR MS. Water Res. 222, 118881 https://doi.org/10.1016/j.watres.2022.118881.

Hur, J., Lee, B.-M., Shin, K.-H., 2014. Spectroscopic characterization of dissolved organic matter isolates from sediments and the association with phenanthrene binding affinity. Chemosphere 111, 450–457. https://doi.org/10.1016/j.chemosphere.2014.04.018.

Ju, Y., Liu, C., Ganiyu, S.O., Zhao, Y., Gamal El-Din, M., 2023. Electrochemical degradation of dissolved organic matters in oil sands process water using continuous-flow packed bed electrode reactor. Sep. Purif. Technol. 320, 124135 https://doi.org/10.1016/j.seppur.2023.124135.

Kaboudin, B., Behroozi, M., Sadighi, S., 2022. Recent advances in the electrochemical reactions of nitrogen-containing organic compounds. RSC Adv. 12, 30466–30479. https://doi.org/10.1039/D2RA04087E.

Karnachuk, O.V, Rusanov, I.I., Panova, I.A., Grigoriev, M.A., Zyusman, V.S., Latygolets, E.A., Kadyrbaev, M.K., Gruzdev, E.V, Beletsky, A.V, Mardanov, A.V, 2021. Microbial sulfate reduction by Desulfovibrio is an important source of hydrogen sulfide from a large swine finishing facility. Sci. Rep. 11, 10720.

Kim, W.-S., Park, G.-Y., Kim, D.-H., Jung, H.-B., Ko, S.-H., Baek, K., 2012. In situ field scale electrokinetic remediation of multi-metals contaminated paddy soil: Influence of electrode configuration. Electrochim. Acta 86, 89–95. https://doi.org/10.1016/j.electacta.2012.02.078.

Klik, B.K., Gusiatin, Z.M., Kulikowska, D., 2020. Suitability of environmental indices in assessment of soil remediation with conventional and next generation washing agents. Sci. Rep. 10, 20586. https://doi.org/10.1038/s41598-020-77312-7.

Ksionzek, K.B., Lechtenfeld, O.J., McCallister, S.L., Schmitt-Kopplin, P., Geuer, J.K., Geibert, W., Koch, B.P., 2016. Dissolved organic sulfur in the ocean: biogeochemistry of a petagram inventory. Science (80) 354, 456–459.

Kumar, N., Ramirez-Ortiz, D., Solo-Gabriele, H.M., Treaster, J.B., Carrasquillo, O., Toborek, M., Deo, S., Klaus, J., Bachas, L.G., Whitall, D., 2016. Environmental PCBs in Guánica Bay, Puerto Rico: implications for community health. Environ. Sci. Pollut. Res. 23, 2003–2013.

Kümmel, S., Herbst, F.-A., Bahr, A., Duarte, M., Pieper, D.H., Jehmlich, N., Seifert, J., von Bergen, M., Bombach, P., Richnow, H.H., 2015. Anaerobic naphthalene degradation by sulfate-reducing Desulfobacteraceae from various anoxic aquifers. FEMS Microbiol. Ecol. 91, fiv006.

Kurek, M.R., Poulin, B.A., McKenna, A.M., Spencer, R.G.M., 2020. Deciphering dissolved organic matter: ionization, dopant, and fragmentation insights via Fourier transform-ion cyclotron resonance mass spectrometry. Environ. Sci. Technol. 54, 16249–16259. https://doi.org/10.1021/acs.est.0c05206.

Laszakovits, J.R., Somogyi, A., MacKay, A.A., 2020. Chemical alterations of dissolved organic matter by permanganate oxidation. Environ. Sci. Technol. 54, 3256–3266. https://doi.org/10.1021/acs.est.9b06675.

Lee, W., Westerhoff, P., Croué, J.-P., 2007. Dissolved organic nitrogen as a precursor for chloroform, Dichloroacetonitrile, N-Nitrosodimethylamine, and trichloronitromethane. Environ. Sci. Technol. 41, 5485–5490. https://doi.org/10.1021/es070411g.

Li, X., Zhang, X., Zhao, X., Yu, B., Weng, L., Li, Y., 2019. Efficient removal of metolachlor and bacterial community of biofilm in bioelectrochemical reactors. Appl. Biochem. Biotechnol. 189, 384–395.

Li, X.-G., Cao, H.-B., Wu, J.-C., Yu, K.-T., 2001. Inhibition of the metabolism of nitrifying bacteria by direct electric current. Biotechnol. Lett. 23, 705–709. https://doi.org/10.1023/A:1010346501857.

Liu, Q., Zhang, Q., Jiang, S., Du, Z., Zhang, X., Chen, H., Cao, W., Nghiem, L.D., Ngo, H. H., 2022. Enhancement of lead removal from soil by in-situ release of dissolved organic matters from biochar in electrokinetic remediation. J. Clean. Prod. 361, 132294 https://doi.org/10.1016/j.jclepro.2022.132294.

Lv, J., Zhang, S., Wang, S., Luo, L., Cao, D., Christie, P., 2016. Molecular-scale investigation with ESI-FT-ICR-MS on fractionation of dissolved organic matter induced by adsorption on iron oxyhydroxides. Environ. Sci. Technol. 50, 2328–2336. https://doi.org/10.1021/acs.est.5b04996.

Maini, G., Sharman, A.K., Knowles, C.J., Sunderland, G., Jackman, S.A., 2000. Electrokinetic remediation of metals and organics from historically contaminated soil. J. Chem. Technol. Biotechnol. 75, 657–664. https://doi.org/10.1002/1097-4660(200008)75:8<657::AID-JCTB263>3.0.CO;2-5.

Maqbool, T., Jiang, D., 2023. Electrokinetic remediation leads to translocation of dissolved organic matter/nutrients and oxidation of aromatics and polysaccharides. Sci. Total Environ. 876, 162703 https://doi.org/10.1016/j.scitotenv.2023.162703.

Maqbool, T., Sun, M., Chen, L., Zhang, Z., 2022. Exploring the fate of dissolved organic matter at the molecular level in the reactive electrochemical ceramic membrane system using fluorescence spectroscopy and FT-ICR MS. Water Res 210, 117979. https://doi.org/10.1016/j.watres.2021.117979.

McCarthy, M., Pratum, T., Hedges, J., Benner, R., 1997. Chemical composition of dissolved organic nitrogen in the ocean. Nature 390, 150–154.

McKee, G.A., Hatcher, P.G., 2015. A new approach for molecular characterisation of sediments with Fourier transform ion cyclotron resonance mass spectrometry: Extraction optimisation. Org. Geochem. 85, 22–31.

Popp, F.D., Schultz, H.P., 1962. Electrolytic reduction of organic compounds. Chem. Rev. 62, 19–40.

Pourfadakari, S., Jorfi, S., Roudbari, A., Javid, A., Talebi, S.S., Ghadiri, S.K., Yousefi, N., 2021. Optimization of electro-kinetic process for remediation of soil contaminated with phenanthrene using response surface methodology. Environ. Sci. Pollut. Res. 28, 1006–1017. https://doi.org/10.1007/s11356-020-10495-8.

Ren, Z.-L., Tella, M., Bravin, M.N., Comans, R.N.J., Dai, J., Garnier, J.-M., Sivry, Y., Doelsch, E., Straathof, A., Benedetti, M.F., 2015. Effect of dissolved organic matter composition on metal speciation in soil solutions. Chem. Geol. 398, 61–69. https://doi.org/10.1016/j.chemgeo.2015.01.020.

Šantl-Temkiv, T., Finster, K., Dittmar, T., Hansen, B.M., Thyrhaug, R., Nielsen, N.W., Karlson, U.G., 2013. Hailstones: a window into the microbial and chemical inventory of a storm cloud. PLoS One 8, e53550.

Schmidt, F., Koch, B.P., Elvert, M., Schmidt, G., Witt, M., Hinrichs, K.-U., 2011. Diagenetic transformation of dissolved organic nitrogen compounds under contrasting sedimentary redox conditions in the black sea. Environ. Sci. Technol. 45, 5223–5229. https://doi.org/10.1021/es2003414.

Smith, D.F., Podgorski, D.C., Rodgers, R.P., Blakney, G.T., Hendrickson, C.L., 2018. 21 tesla FT-ICR mass spectrometer for ultrahigh-resolution analysis of complex organic mixtures. Anal. Chem. 90, 2041–2047.

Tabuchi, K., Kojima, H., Fukui, M., 2010. Seasonal changes in organic matter mineralization in a sublittoral sediment and temperature-driven decoupling of key processes. Microb. Ecol. 60, 551–560. https://doi.org/10.1007/s00248-010-9659-9.

U.S. EPA, 2021. This is superfund: a citizen's guide to EPA's superfund program.

US-EPA, 2021. Superfund | US EPA [WWW Document]. URL https://www.epa.gov/superfund (accessed 9.17.22).

Virkutyte, J., Sillanpää, M., Latostenmaa, P., 2002. Electrokinetic soil remediation — critical overview. Sci. Total Environ. 289, 97–121. https://doi.org/10.1016/S0048-9697(01)01027-0.

Wang, J., Xie, Q., Xiang, Y., Xue, J., Jiang, T., Zhang, C., Li, J., Wang, Y., Wang, D., 2024. Anthropogenic activities enhance mercury methylation in sediments of a multifunctional lake: Evidence from dissolved organic matter and mercury-methylating microorganisms. J. Hazard. Mater. 466, 133505 https://doi.org/10.1016/j.jhazmat.2024.133505.

Wang, S., Guo, S., Li, F., Yang, X., Teng, F., Wang, J., 2016. Effect of alternating bioremediation and electrokinetics on the remediation of n-hexadecane-contaminated soil. Sci. Rep. 6, 23833. https://doi.org/10.1038/srep23833.

Wen, D., Fu, R., Li, Q., 2021. Removal of inorganic contaminants in soil by electrokinetic remediation technologies: A review. J. Hazard. Mater. 401, 123345 https://doi.org/10.1016/j.jhazmat.2020.123345.

Xu, H., Guo, L., Jiang, H., 2016. Depth-dependent variations of sedimentary dissolved organic matter composition in a eutrophic lake: Implications for lake restoration. Chemosphere 145, 551–559. https://doi.org/10.1016/j.chemosphere.2015.09.015.

Xu, S., Guo, S., Wu, B., Li, F., Li, T., 2014. An assessment of the effectiveness and impact of electrokinetic remediation for pyrene-contaminated soil. J. Environ. Sci. 26, 2290–2297. https://doi.org/10.1016/j.jes.2014.09.014.

Yang, L., Choi, J.H., Hur, J., 2014. Benthic flux of dissolved organic matter from lake sediment at different redox conditions and the possible effects of biogeochemical processes. Water Res. 61, 97–107. https://doi.org/10.1016/j.watres.2014.05.009.

Yuan, F., Chaffin, J.D., Xue, B., Wattrus, N., Zhu, Y., Sun, Y., 2018. Contrasting sources and mobility of trace metals in recent sediments of western Lake Erie. J. Great Lakes Res. 44, 1026–1034. https://doi.org/10.1016/j.jglr.2018.07.016.

Yuan, T., Yuan, Y., Zhou, S., Li, F., Liu, Z., Zhuang, L., 2011. A rapid and simple electrochemical method for evaluating the electron transfer capacities of dissolved organic matter. J. Soils Sediments 11, 467–473. https://doi.org/10.1007/s11368-010-0332-1.

Zhang, B., Wang, X., Fang, Z., Wang, S., Shan, C., Wei, S., Pan, B., 2021. Unravelling molecular transformation of dissolved effluent organic matter in UV/H2O2, UV/persulfate, and UV/chlorine processes based on FT-ICR-MS analysis. Water Res 199, 117158. https://doi.org/10.1016/j.watres.2021.117158.

Zhang, C., Zhu, M., Zeng, G., Yu, Z., Cui, F., Yang, Z., Shen, L., 2016. Active capping technology: a new environmental remediation of contaminated sediment. Environ. Sci. Pollut. Res. 23, 4370–4386. https://doi.org/10.1007/s11356-016-6076-8.

Zhang, L., Sun, Q., Dou, Q., Lan, S., Peng, Y., Yang, J., 2022. The molecular characteristics of dissolved organic matter in urbanized river sediments and their environmental impact under the action of microorganisms. Sci. Total Environ. 154289 https://doi.org/10.1016/j.scitotenv.2022.154289.

Zhang, W., Wu, Y., Wu, J., Zheng, X., Chen, Y., 2022. Enhanced removal of sulfur-containing organic pollutants from actual wastewater by biofilm reactor: Insights of sulfur transformation and bacterial metabolic traits. Environ. Pollut. 313, 120187 https://doi.org/10.1016/j.envpol.2022.120187.

Zheng, Y., Li, H., Yu, Q., Yu, L., Jiao, B., Li, D., 2021. Application of UV radiation for in-situ Cr(VI) reduction from contaminated soil with electrokinetic remediation. J. Hazard. Mater. 416, 125806 https://doi.org/10.1016/j.jhazmat.2021.125806.